

SPIRAL CHEMICAL SHIFT IMAGING AT 3T USING 32 CHANNEL RECEIVE ARRAY AND ONLINE RECONSTRUCTION

Gagoski Aleksandar Borjan

*Department of Electrical Engineering and Computer Science,
Massachusetts Institute of Technology, Cambridge, MA, USA*

Abstract: Magnetic resonance spectroscopic imaging (MRSI) is an imaging technique where one obtains a spectrum of signals, e.g. brain metabolites *in vivo*, from particular spatial locations of interest. Conventional MRSI suffers from intrinsically long acquisition times, making this technique suitable for *in vivo* acquisitions only for modest spatial resolutions. Spiral MRSI is a fast encoding algorithm that plays spiral-shaped k-space trajectories repeatedly within one repetition period (TR), therefore sampling the (k_x, k_y, k_t) space simultaneously. This offers two orders of magnitude decrease in acquisition time compared to the conventional MRSI, at no SNR cost. In this work we show implementation of the spiral MRSI algorithm on Siemens' MRI platform, and present results from *in vivo* experiments on healthy volunteers.

Key words: magnetic resonance imaging, spiral spectroscopic imaging, fast spectroscopic imaging.

1. Introduction

MRI is a great tool not only because it enables informative structural imaging, but also due to the fact that it offers possibilities for monitoring biochemistry *in vivo*. Magnetic Resonance Spectroscopic Imaging (MRSI), also known as chemical shift imaging (CSI), is an imaging technique where one obtains a spectrum of signals, e.g. brain metabolites *in vivo*, from an isolated volume of tissue. MRSI is based on the MR phenomenon of chemical shift, a subtle frequency shift in the signal that is dependent on the chemical environ-

ment of the particular compound. It is due to this frequency shift that there is a potential for physiological evaluation and material characterization of a volume of interest.

Chemical shift is defined as a small displacement of the resonance frequency due to shielding created by the orbital motion of the surrounding electrons in response to the main B_0 field. By placing a sample of biological tissue in a uniform magnet, exciting it, recording its free induction decay (FID), and then Fourier transforming the FID, the resultant MR spectrum shows resonances at different frequencies corresponding to different chemical shifts. The amount of displacement and the amplitude of the peaks in the spectrum depend on the molecular structure of the compound of interest. Being in a presence of B_0 , the effective field experienced by the nucleus is $B_{eff} = B_0 - B_{0\sigma}$. Further, bearing in mind that ω is proportional to B_0 (the Larmor relationship), we have that

$$\omega_{eff} = \omega_0 - \omega_{0\sigma} = \omega_0(1 - \sigma) \quad (1.1)$$

where σ equals the shielding constant that depends on the chemical environment, and therefore $\omega_{0\sigma}$ is the displacement of the resonance frequency. From this, it can be concluded that *the change in frequency is proportional to the strength of the main magnetic field B_0* .

The frequency axis in MRSI, for historical reasons, is such that the frequency decreases from left to right and is given in units of “parts per million” or p.p.m. The chemical shift is defined with respect to a reference frequency ω_r . If the resonance frequency of the sample of interest is ω_s , the chemical shift δ , in p.p.m units (using (1.1) is:

$$\delta = \frac{\omega_s - \omega_r}{\omega_r} \cdot 10^6 = \frac{\omega_0(1 - \sigma_s) - \omega_0(1 - \sigma_r)}{\omega_0(1 - \sigma_r)} \cdot 10^6 = \frac{\sigma_r - \sigma_s}{1 - \sigma_r} \cdot 10^6 \approx \boxed{(\sigma_r - \sigma_s) \cdot 10^6} \quad (1.2)$$

where the last approximation is due to the fact that $\sigma_r = 1$

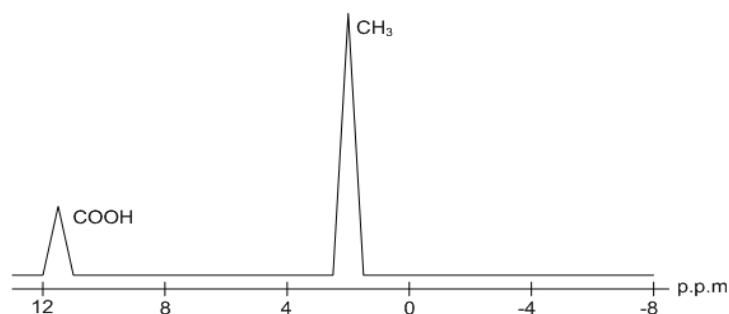


Figure 1-1 – ^1H MR spectrum of acetic acid (CH_3COOH) showing the effects of the chemical shift phenomenon. The COOH group experiences different effective B_0 magnetic field compared to the CH_3 group

Слика 1-1 – ^1H спектрум од магнетна резонанса на оцетина киселина (CH_3COOH), на кој се прикажуваат ефектите од феноменот на хемиско поместување. Молекуларната група COOH е стимулирана од различно ефективно B_0 магнетно поле споредено со полето кое го чувствува молекуларната група CH_3

A schematic ^1H spectrum is given in Figure 1-1. Due to the fact that the valency of the oxygen in the COOH group leads to an attraction of the electron away from the proton, there is less shielding for the proton in the COOH group compared to the proton in the CH_3 group. This is why COOH deviates more from the reference frequency (positioned at 0 p.p.m), compared to CH_3 .

In this article we present ^1H spectra of the human head using time-efficient sampling schemes using spiral-shaped k-space trajectories. However, it is worth mentioning that ^{13}C and ^{31}P CSI is of significant importance. For example, ^{31}P spectra are used for obtaining quantitative information about chemical compounds like adenosine triphosphate (ATP), phosphocreatine (PCr), and inorganic phosphate (P_i). However, ^{13}C and ^{31}P spectra have a significantly lower signal-to-noise ratio (SNR) compared to ^1H spectra and therefore are more difficult to detect and quantify. This is mainly because of lower abundance and sensitivity for these nuclei.

2. Conventional phase-encoded CSI

Before giving a brief overview of the conventional CSI and laying down its advantages and disadvantages, together with the motivation for improvement, it is instructive to review the derivation of the signal equation for the

case of spectroscopic imaging. The derivation presented closely followed that of Dwight Nishimura [1].

Leaving out the frequency axis for the time being, and considering only a three-dimensional (3D) space of interest, one can imagine a tiny “magnetic oscillator” rotating at a frequency $\omega = \gamma \cdot B$ (γ is the gyromagnetic ratio and B is the main magnetic field) at each spatial location (x, y, z) . Modeling these magnetic oscillators as having (constant in time) magnitude $m(x, y, z)$ and (variable in time) phase $\phi(x, y, z, t)$, the signal seen by the receive coils, i.e. the transverse magnetization, is given by

$$s(t) = \int_x \int_y \int_z m(x, y, z) \cdot e^{-i\phi(x, y, z, t)} dx dy dz \quad (2.3)$$

Bearing in mind that frequency is the time rate of change in phase, and that it is proportional to the applied field $B(x, y, z, t)$, one can write the following:

$$\phi(x, y, z, t) = \int_0^t \frac{d}{dt} \phi(x, y, z, \tau) d\tau = \int_0^t \omega(x, y, z, \tau) d\tau = \gamma \int_0^t B(x, y, z, \tau) d\tau \quad (2.4)$$

knowing that $B(x, y, z, t) = B_0 + G_x(t)x + G_y(t)y + G_z(t)z$ and that k-space is defined as the time integral of the gradients, i.e.

$$k(t) = \frac{\gamma}{2\pi} \int_0^t G(\tau) d\tau, \quad (2.5)$$

the signal equation given in (2.3) becomes

$$s(t) = \int_x \int_y \int_z m(x, y, z) \cdot e^{-i[k_x(t)x + k_y(t)y + k_z(t)z]} dx dy dz \quad (2.6)$$

The difference between (2.6) and the signal equation in MRSI, is the consideration of a frequency axis in order to account for the chemical shift phenomenon. Therefore, defining $k_f(t) = t$, the signal equation in MRSI becomes

$$s(t) = \int_x \int_y \int_z \int_f m(x, y, z, f) \cdot e^{-i[k_x(t)x + k_y(t)y + k_z(t)z + k_f(t)f]} dx dy dz df \quad (2.7)$$

Equation (2.7) is a four-dimensional (4D) Fourier Transform (FT) of the excited object and its spectral contents. From this, it is clear that the in-

clusion of the temporal variable adds another dimension to the imaging problem compared to structural imaging. This formulation clearly depicts volumetric CSI acquisition and reconstruction as a four-dimensional sampling problem.

2.1. Challenges in MRSI

The main constraint in MRSI comes from the fact that the signals of the metabolites that we are interested in are orders of magnitude lower compared to the signals coming from the water and the lipids. The concentration of the water molecules is approximately 55 M, and those of the metabolites of interest are less than 10 mM [2]. This fact is the main reason why MRSI scans have intrinsically low SNR compared to conventional MRI of water. Figure 2–1 shows that compared to subcutaneous fat signals near the brain, the metabolite spectra are much lower and present a large dynamic range between the desired metabolites and the artifact signals from fat.

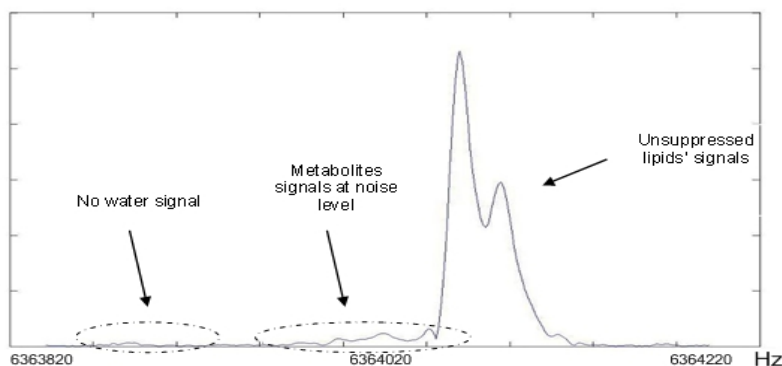


Figure 2–1 – Spectrum from a voxel located near a lipid tissue at 1.5 Tesla system. The lipids' signal was not suppressed at all. The signals of the metabolites (shown with the arrow) are in the noise level, and therefore this spectrum is useless ($T1/TE/TR = N/A/288 \text{ ms}/2 \text{ s}$; Acquisition time = 24 seconds; 1.5 cm thick slice and no encoding in (x,y))

Слика 2–1 – Спектърум од пиксел лоциран во близина на масно ткиво добиен од 1.5 Тесла МР систем. Сигналој од масниите војштии не беше појаснајќи. Метаболичкиите сигнали (идентифкувани со стрелкајќа) се на нивојто на шумој, поради што овој спектърум е безвреден. Во случајов, времето на ехојто (TE) е 288 ms, повторувачкиој интервал (TR) е 2 s. Времето појребно за аквизиција е 24 секунди; Дебелинајта на стимулираната површина е 1.5 cm без никакво енкодирање во (x,y) просјорој

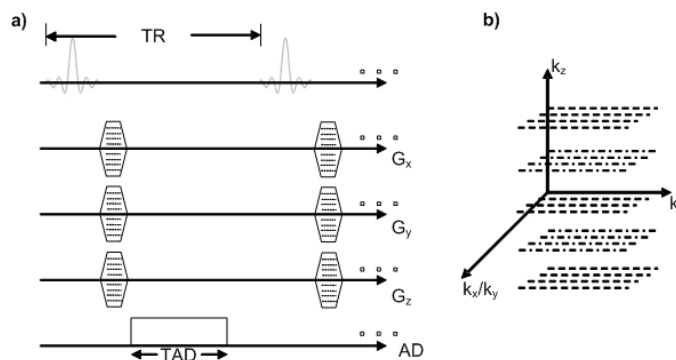


Figure 2-2 – Conventional MRSI. a) timing diagram; b) (k_x, k_y, k_z, k_f) encoding
 Слика 2-2 – Конвенционално сџектроскојско снимање со магнетна резонанса
 (CCMP). a) временски дијаграм; b) Енкодирање во (k_x, k_y, k_z, k_f) простор

Furthermore, main field inhomogeneities may additionally lower the SNR in MRSI and complicate signal detection and quantification. Any undesirable variations in the main magnetic field B_0 will cause a shift along the frequency axis, causing overlap of the metabolites' peaks and creating ambiguity in metabolites' identification. These main field inhomogeneities are mainly due to susceptibility effects within the body near the boundaries of air and tissue, and thus vary from one subject to another.

2.2. Conventional CSI

A straightforward way of doing spectroscopic imaging is to do the following (in order, and per repetition time, TR) [3, 4]: excite the volume of interest, “travel” to a certain (k_x, k_y, k_z) position by applying short gradient lobes of appropriate area and “stop”, turn the Analog to Digital Converter (ADC) on, and finally, record the free induction decay signal (FID). This is to be repeated for all (k_x, k_y, k_z) locations of interest. The number of repetition times will depend on the Field of View (FOV) and the spatial resolution requirements. This is pictorially depicted in Figure 2-2.

A typical single voxel spectrum is given in Figure 2-3. In this figure it is clear that the water and lipid signals have been significantly suppressed. In order to suppress the water signal, spectrally selective RF pulses [5] (a spin-

echo pair) are used in this particular sequence design. These pulses act like a band-pass filter along the k_f axis: the frequency of the water signal is in their stop band, but the frequencies of the lipid signal are in their pass band mainly because at field strengths lower than 3T, the lipid signals and the metabolite signals are spectrally close.

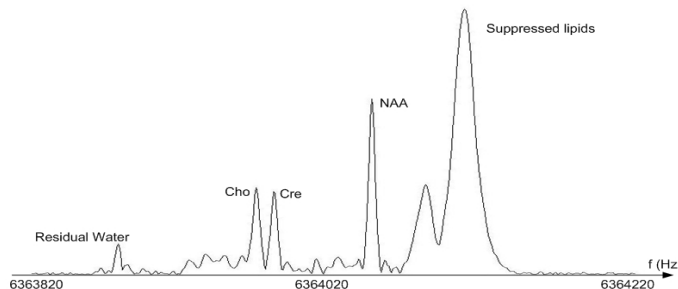


Figure 2-3 – A typical single voxel spectrum of the human head. The above spectrum is obtained on a 1.5T system using conventional MRSI ($TI/TE/TR = 171ms/288ms/2s$;

Acquisition time = 24 seconds; 1.5 cm thick slice and no encoding in (x,y)

Слика 2-3 – Типичен спектар од еден воксел во човечка глава. Испитој е добиен од 1.5 Тесла МР систем, користејќи конвенционална ССМР ($TE = 288ms$; $TR = 2s$; време на инверзија (TI) = 171ms;). Времето потребно за аквизиција е 24 секунди; Дебелината на стимулираната површина е 1.5cm без никаво енкодирање во (x,y) просјорној

As mentioned, MRSI suffers from intrinsically low SNR. Since SNR in MRI is proportional to the acquisition time and the voxel size [6, 7], i.e.

$$SNR \propto V_{size} \cdot \sqrt{T_{AD}}, \quad (2.8)$$

in order to improve SNR, one could increase the voxel volume, or acquisition time, or both. Moreover, voxel size depends on the spatial resolution (lower spatial resolution gives larger voxel size), and, further, the number of (k_x, k_y, k_z) encodes depends on the FOV and spatial resolution parameter. Having said this, it can be concluded that *FOV, spatial resolution and imaging time are not independent parameters in conventional MRSI*. This is the main reason for one of the biggest disadvantages in conventional MRSI – the inflexible coupling between scan time and resolution parameters. As an example, a volumetric scan that encodes a volume at a modest 16^3 k-space locations with $TR = 2s$ takes about 2 hours and 20 minutes, a prohibitive scan time for in vivo examinations.

3. In vivo spiral chemical shift imaging

In conventional CSI, spectral bandwidth is said to be “free” since the ADC design on the current MRI systems allows temporal sampling of as low as $0.1\mu\text{s}$, corresponding to a very wide spectral bandwidth of 10MHz. However, on 1.5 Tesla systems, the metabolites of interest span frequencies that are within a spectral range of 400Hz. This implies that 400Hz, corresponding to temporal sampling of 2.5ms, is a sufficient spectral bandwidth for the purposes of MRSI – temporal sampling at less than 2.5ms per point is not logical since it does not provide any more information about the proton metabolites of interest.

These facts open the doors for the development of a CSI algorithm that is more efficient than the phase encoded CSI scheme. Furthermore, the hardware of the gradients has undergone major improvements in recent years, allowing possibilities for very fast k-space traversing. Nevertheless, the conventional CSI takes absolutely no advantage of the gradients’ potential, suggesting that efficient k-space sampling with time-varying gradients could be a method to overcome the rigid constraints on minimum acquisition time in phase-encoded CSI. In addition as noted in (2.8) and [6, 7], it can be seen that *the SNR does not depend on the number of voxels*. This fact, combined with the ability for fast k-space sampling, provides the basis for the development of fast CSI algorithms using time-varying gradients.

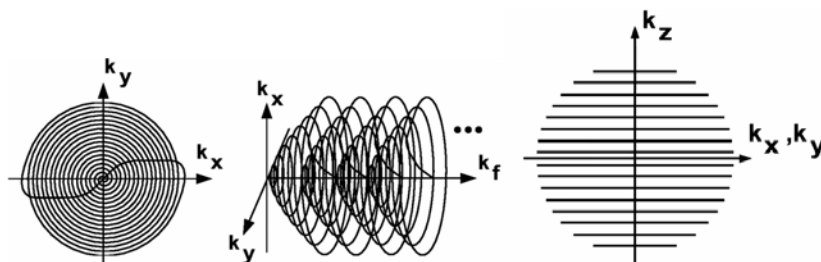


Figure 3–4 – Simultaneous encoding along, k_f axes. Every (k_y, k_z) point is separated by τ_s , along the k_f axis. For volumetric acquisitions, phase encoding along k_z is performed

Слика 3–4 – Симултано енкодираније дољж k_f оскатија. Секоја тачка во (k_y, k_z) проспорој е разделена во интервал од τ_s , дољж k_f оскатија. За волуменјриски аквизицији се применува фазно енкодираније дољж k_z оскатија

Many authors have touched upon the theory and application of applying time-varying gradients during the readout of a spectroscopic acquisition [8–16]. The two most widely used algorithms that improve the time efficiency of CSI

experiments are based on echo-planar and spiral trajectories played repeatedly in a rather long acquisition time (~200ms–450ms). This article will concentrate its discussion around the spiral chemical shift imaging.

3.1. Spiral CSI, ultra time-efficient sampling scheme

Originally introduced by Adalsteinsson *et al.* [9], spiral CSI is a fast spectroscopic imaging algorithm that offers two orders of magnitude decrease in acquisition times compared to the conventional PE CSI. This encoding scheme samples the (k_x, k_y, k_f) space simultaneously within one TR, by repeatedly playing spiral trajectories along the x and y gradients in a rather long readout period (300ms–400ms), as shown in Figure 3–4. For volumetric acquisitions, phase encoding is performed along the k_z axis. Given a small *spatial* FOV and/or low *spatial* resolution, it is possible to design a spiral trajectory that has a length less than, or equal to the temporal sampling rate τ_s , needed to satisfy the spectral bandwidth constraints (as noted previously, for 1.5T systems, this is 2.5ms, corresponding to 400Hz of spectral BW). This means that, for the given special case, one is able to obtain single slice spectroscopy data in *only one TR!*

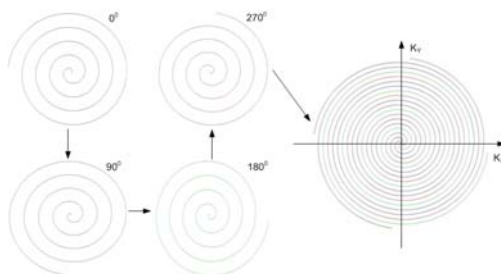


Figure 3–5 – Angular (0° , 90° , 180° , 270°) interleaves ($N_A = 4$). The final k -space trajectory is four times as dense as each individual interleaf

Слика 3–5 – Аголни (0° , 90° , 180° , 270°) сеџменїи ($N_A = 4$). Крајнаїа k -їросїорна їтраекїорїја е чеїири їаїїи їоџусїїа од ѳусїїинаїїа на еден сеџменїи

However, for more realistic spatial resolution and FOV parameters it is almost always impossible to traverse certain k -space volume in time τ_s . Furthermore, the value of τ_s is inversely proportional to the field strengths (higher field strengths give wider spectral bandwidth constraints). That means that within one TR *only gaps of the desired* k -space are acquired, and the rest of the “unfilled” k -space data is obtained in subsequent TRs. In other words, the

desired k-space spiral trajectory is divided, or decomposed into spiral trajectories (angular interleaves) that are sparser than the original, and are not longer than τ_s . The concept of interleaving is shown in Figure 3–5, for the case for $N_A = 4$ angular interleaves, meaning that for this particular k-space trajectory (i.e. spatial FOV and resolution), the spiral CSI scan would last four repetition periods.

Table 1 – Табела 1

Comparison between the acquisition times of spiral and PE CSI for two different sets of imaging parameters

Споредба између времена потребно за аквизиција на спирално и конвенционално ССМР, за две различне групе на параметри

	(x,y): (32 × 32); FOV _{XY} = 24cm; 800Hz spectral BW	(x,y,z): (32 × 32 × 32); FOV _{XY} = 24cm; 800Hz spectral BW
Conventional CSI	34.13 min	1092.27 min (~18.2h)
Spiral CSI	0.267 min	5.8 min
Conv./Spiral CSI	~128	~188

Spiral CSI trades off spatial in-plane field of view (FOV_{XY}) with spectral bandwidth. This means that for a fixed spatial FOV and spatial resolution, going to a higher field means an inherent increase in scan time. However, even when comparing the imaging times for ultra high field (e.g. 7T) spectroscopic imaging, the spiral CSI still provides orders of magnitude, the two orders increase in time efficiency compared to PE CSI. Table 1 compares the acquisition times between spiral and PE CSI for two specific imaging parameters, where the time efficiency is evident.

Having inherently low SNR, spectroscopic imaging takes great advantage of receive arrays with a large number of coil elements as they provide significant SNR improvement. 32-channel receive arrays are becoming a standard, and 64-, 96- and even 128-channel arrays are in development. The major challenge when reconstructing spiral CSI data is the immense amount of data, particularly when using a large number of coils. Therefore, the time efficiency provided by the spiral CSI comes at a cost of high-capacity receiver pipeline, and non-trivial trajectory designs and reconstruction algorithms. Since the spirally acquired data is non-uniformly sampled, the gridding algorithm is usually used to resample the data points on a rectangular grid which can then be easily fast-Fourier-transformed. The gridding procedure is nothing more than an interpolation (or convolution) of the spiral samples with a specified kernel (e.g. Kaiser-

Bassel window). This process can be time-consuming, since it has to be done for the spiral data at every sample point along the k_f (or the time) axis and for every coil element used.

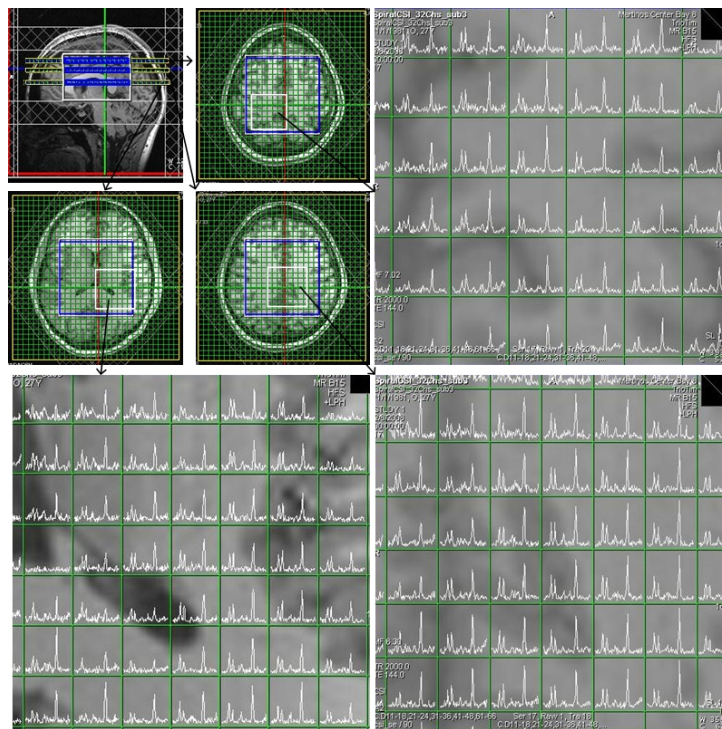


Figure 3-6 – Magnitude spectra from three different slices and regions acquired in 13.5 minute long spiral CSI scan with isotropic voxel size of 0.216 cc using 32-channel coil array

Слика 3-6 – Спектърум на магнитудите од три различни делови од мозокој, добиени за 13.5 минути со помош на аквизиција од спиралнојо ССМР. Големината на изотројскијте џксели е 0.216 cm^3 корисителјки 32-канална намотјка за џримање на сигналот

However, using the capabilities of the most recent hardware and software, online reconstruction of the spiral CSI using a large number of receive elements is possible in clinical settings. Figure 2.6 shows spectroscopy data at 3T from three slices of an *in vivo* volumetric (32 phase-encoded slices) spiral CSI scan acquired using 32-channel receive coil array in 13.5 minutes (2 averages) and an isotropic voxel size of *only* 0.216cc (TE = 144ms, TR = 2s). PRESS excitation scheme was used to excite a box of size (x, y, z) = 8 × 9 × 6cm posi-

tioned wholly within the brain. The spectra (overlaid on high resolution structural images) present a great SNR of the three major metabolites of interest (NAA, Crue and Cho) even with the relatively short acquisition time and small voxel size.

Being able to acquire volumetric spectroscopic data with a high enough spatial resolution, opens possibilities for creating metabolite maps, i.e. images obtained by estimating the spatial distribution of a particular metabolite. Figure 2–7 shows an example of metabolite maps for the three major metabolites in the human brain: N-acetyl aspartate (NAA), creatine (Cr) and Choline (Ch). Each image is obtained by performing a linear least square fit along the frequency axis for each spatial location.

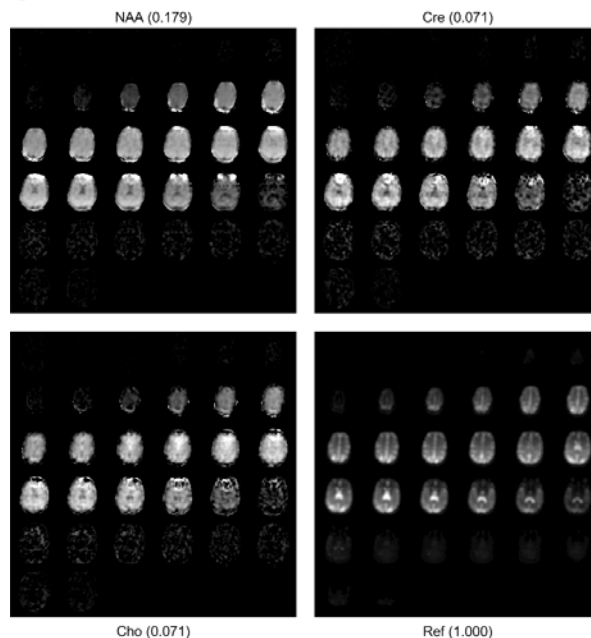


Figure 3–7 – NAA, Cre, Cho and on-resonance (water) maps from a 3D volumetric 4-channel acquisition. The first three are obtained from the 15 minutes metabolite scans, whereas the last one is obtained from the 4 minutes reference scan. The numbers shown represent the absolute scaling of a map relative to the rest of the maps

Слика 3–7 – Стандардна структурна слика од мозоког и просторни мапи на трије мозочни метаболити (NAA, Cre, Cho), добиени од тридимензионална, волуметриска аквизиција корисјејки 4-канална намојка. Структурна слика е добиена од 4 минутен референен скен, додека метаболитскије мапи се добиени од 15 минутни аквизицији. Прикажаније броеви прејстававааји ајсолујно одмерување на одреденаја мапи во споредба со осјанајније

4. Conclusion

We have developed and implemented the spiral CSI algorithm with online gridding reconstruction [17] on Siemens scanners, and were therefore able to acquire reliable *in vivo* spectroscopic data on healthy volunteers. Receive arrays with a large number of coil elements offer excellent benefits for volumetric, time-efficient spiral CSI. The results shown in this work illustrate that 3D volumetric CSI with 0.225-cc voxels in less than 15 minutes yield good spectral quality and SNR. Future work on minimal oversampling [17] and multi-threaded reconstruction among the 8 available processors will significantly reduce the reconstruction time. This work sets up the basis for usage of chemical shift imaging as a diagnostic tool for many neurodegenerative diseases by providing metabolite quantification at high spatial resolution. Appended to excitation schemes that provide improved spectral-spatial target profiles (e.g. parallel RF transmission) using RF waveforms with short durations, spiral CSI can provide a critical contribution towards providing important information about metabolite quantities in hard-to-get brain regions, like cortical areas near the skull and/or the spinal cord.

REFERENCES

1. Nishimura D.G. (1996): Principles of magnetic resonance imaging.
2. Pan J.W. et al. (1991): Quantitation of metabolites by ^1H NMR. *Magn Reson Med*, 20(1): p. 48–56.
3. Brown T.R., Kincaid B.M. and Ugurbil K. (1982): NMR chemical shift imaging in three dimensions. *Proc Natl Acad Sci U S A*, 79(11): p. 3523–6.
4. Howe F.A. et al. (1993): Proton spectroscopy in vivo. *Magn Reson Q*, 9(1): p. 31–59.
5. Meyer C.H. et al. (1990): Simultaneous spatial and spectral selective excitation. *Magn Reson Med*, 15(2): p. 287–304.
6. Macovski A. (1996): Noise in MRI. *Magn Reson Med*, 36(3): p. 494–7.
7. Edelstein W.A. et al. (1986): The intrinsic signal-to-noise ratio in NMR imaging. *Magn Reson Med*, 3(4): p. 604–18.
8. Macovski A. (1985): Volumetric NMR imaging with time-varying gradients. *Magn Reson Med*, 2(1): p. 29–40.
9. Adalsteinsson E. et al. (1998): Volumetric spectroscopic imaging with spiral-based k-space trajectories. *Magn Reson Med*, 39(6): p. 889–98.
10. Haase A. and Matthaei D. (1987): Spectroscopic FLASH Imaging (SPLASH imaging). *Journal of Magnetic Resonance*, 71: p. 550–553.

11. Mansfield P. (1984): Spatial mapping of the chemical shift in NMR. *Magn Reson Med*, 1(3): p. 370–86.
12. Matsui S., Sekihara K. and Kohno H. (1985): High-speed spatially resolved NMR spectroscopy using phase-modulated spin-echo trains. Expansion of the spectral bandwidth by combined use of delayed spin-echo trains. *Journal of Magnetic Resonance*, 64: p. 161–171.
13. Matsui S., Sekihara K. and Kohno H. (1985): High-speed spatially resolved high-resolution NMR spectroscopy. *Journal of the American Chemical Society*, 107: p. 2817–2818.
14. Twieg D.B. (1985): Acquisition and accuracy in rapid NMR imaging methods. *Magn Reson Med*, 2(5): p. 437–52.
15. Twieg D.B. (1989): Multiple-output chemical shift imaging (MOCSI): a practical technique for rapid spectroscopic imaging. *Magn Reson Med*, 12(1): p. 64–73.
16. Webb P., Spielman D. and Macovski A. (1989): A fast spectroscopic imaging method using a blipped phase encode gradient. *Magn Reson Med*, 12(3): p. 306–15.
17. Beatty et al. *IEEE Transactions on Medical Imaging*, 24(6), 2005

Резиме

СПИРАЛНО СПЕКТРОСКОПСКО СНИМАЊЕ НА ЗТ СО 32-КАНАЛНА НАМОТКА И ОНЛАЈН РЕКОНСТРУКЦИЈА

Гагоски Александар Борјан

*Department of Electrical Engineering and Computer Science,
Massachusetts Institute of Technology, Cambridge, MA, USA*

Апстракт: Спектроскопското снимање со магнетна резонанса (ССМР) е техника со која се добиваат спектри од сигнали, т.е. мозочни метаболитски записи, од определени просторни локации од интерес. Конвенционалното ССМР како техника бара долги аквизициски времиња, со тоа правејќи ја оваа техника поволна само за *in-vivo* скенирања со скромна резолуција во просторот. Спиралното ССМР е алгоритам за брзо енкодирање, кое користи спирално обликувани k -просторни траектории, кои се повторуваат повеќе пати во еден возбудувачки интервал, и со тоа вршат одмерување на (k_x, k_y, k_t) просторот истовремено. На овој начин, споредено со конвенционалното ССМР, времето потребно за аквизиција се намалува за два реда на големина, притоа без никаква цена врз односот помеѓу сигналот и шумот. Во овој труд се прикажани имплементацијата на алгоритмот за

спирално ССМР на Siemens-ов апарат за магнетна резонанса, како и резултати од in-vivo експерименти направени на здрави волонтери.

Клучни зборови: снимање со магнетна резонанса, спирално спектроскопско снимање, брзо спектроскопско снимање.

Corresponding Author:

Borjan Gagoski
Department of Electrical Engineering
and Computer Science,
Massachusetts Institute of Technology
77 Massachusetts Avenue,
Building 36-776a
Cambridge, MA, 02139
Phone: (617)324-1738
Fax: 617)324-3433

E-mail: gagoski@mit.edu